Earth and Space Science

RESEARCH ARTICLE
10.1029/2019EA000661

Inducing Factors and Impacts of the October 2017 California Wildfires

Andy X. Li[1], **Yuan Wang**[2], **and Yuk L. Yung**[2]

[1]Clements High School, Sugar Land, TX, USA, [2]Division of Geological and Planetary Sciences, California Institute of Technology, Pasadena, CA, USA

Key Points:
- Temporal variations of atmospheric variables are analyzed, which suggest that surface temperature increases while cloud water contents and precipitation decrease in the past 39 years in California
- Higher temperatures, higher surface pressures, lower cloud water contents and precipitation, enhanced Santa Ana winds and sinking air have set up favorable meteorological conditions for stronger wildfires in California
- We provide the first quantitative characteristics of the impact of wildfires on atmospheric CO2, in which the concentration of CO2 is found to increase 2 ppm after the October 2017 California wildfires

Supporting Information:
- Supporting Information S1

Correspondence to:
A. X. Li,
andy122020@gmail.com

Citation:
Li, A. X., Wang, Y., & Yung, Y. L. (2019). Inducing factors and impacts of the October 2017 California wildfires. *Earth and Space Science*, *6*, 1480–1488. https://doi.org/10.1029/2019EA000661

Received 6 APR 2019
Accepted 30 JUL 2019
Accepted article online 4 AUG 2019
Published online 27 AUG 2019

Abstract The California wildfires of October 2017 were one of the largest wildfires in the state's history. Using surface temperature, surface pressure, cloud liquid and ice water contents, precipitation data, and wind data, we explore possible reasons for the wildfires. It is found that the mean surface temperature in California has increased, while mean cloud water contents and mean precipitation in California has decreased over the past 39 years. Higher temperatures, higher surface pressures, lower cloud water contents, lower precipitation, enhanced surface Santa Ana winds, and enhanced sinking air have set up favorable meteorological conditions for stronger wildfires in California, such as the October 2017 wildfires. Furthermore, the CO_2 data from the Orbiting Carbon Observatory 2 satellite have, for the first time, made it possible for us to quantitatively characterize the impact of wildfires on atmospheric CO_2 in California, which revealed that atmospheric CO_2 increased by 2 ppm after the October 2017 California wildfires. Analyses in this study can help us better understand the causes and impacts of wildfires.

1. Introduction

As a response to rising greenhouse gases, air temperature increases over the global domain (Intergovernment Panel on Climate Change, 2013), which can further increase the abundance of water vapor in the atmosphere following the Clausius-Clapeyron relationship (Kao et al., 2018; Li et al., 2011; Santer et al., 2007; Trenberth et al., 2005). Unlike the impact on atmospheric moisture, the influence of global warming on precipitation is more complex. It is found that precipitation increases in wet areas and decreases in dry areas, which is called "wet-get-wetter and dry-get-drier" mechanism (e.g., Allan & Soden, 2007; Chou & Neelin, 2004; Kao et al., 2017; Kao et al., 2018; Li et al., 2011; Polson et al., 2013; Su et al., 2017; Trammell et al., 2015; Wang et al., 2016). The "dry-get-drier" mechanism affects the droughts in the southwestern United States. The air is dry in summer over the southwestern United States, for the Pacific high pressure moves moist air away from this region. In recent years, the air has become dryer and more severe droughts have happened over the southwestern States (Crockett & Westerling, 2018; Griffin & Anchukaitis, 2014). It is also found that droughts in the western United States cover a greater area in recent years than earlier years (Crockett & Westerling, 2018).

In principle, severe droughts could favor wildfires (e.g., Balling et al., 1992; Pausas and Fernandez-Munoz, 2012). In this study, we will explore possible meteorological inducing factors for recent wildfires in California. The October 2017 California wildfires were one of largest wildfires in the state's history. It included ~9,000 wildfires, 1.2 million burned acres, and more than 10,000 destroyed structures. We will use the 2017 wildfires as an example to examine the factors favoring large wildfires in California.

The relationship between the environment and wildfires is interactive. Wildfires affect the environment in many aspects, for example, air quality (Cai et al., 2016). Here we investigate the impact of such wildfires on the concentration of atmospheric CO_2, a well-known greenhouse gas. The impacts of fires on atmospheric CO_2 have been investigated in previous studies (e.g., Guyon et al., 2005; Heymann et al., 2017; O'Shea et al., 2013). Guyon et al. (2005) explored CO_2 emission from Amazonian deforestation fires using aircraft and noticed that there were more CO_2 emitted from forest fires compared with surrounding areas. O'Shea et al. (2013) utilized airborne measurements over eastern Canada and found that these fires released 1,512 g/(kg dry matter) of CO_2 to the atmosphere. Recently, Heymann et al. (2017) utilized CO_2 retrievals from a satellite and found that fires released more CO_2 to the atmosphere over Indonesia compared with its surrounding areas. The global data sets of satellite CO_2 can help us understand the impact of fires on

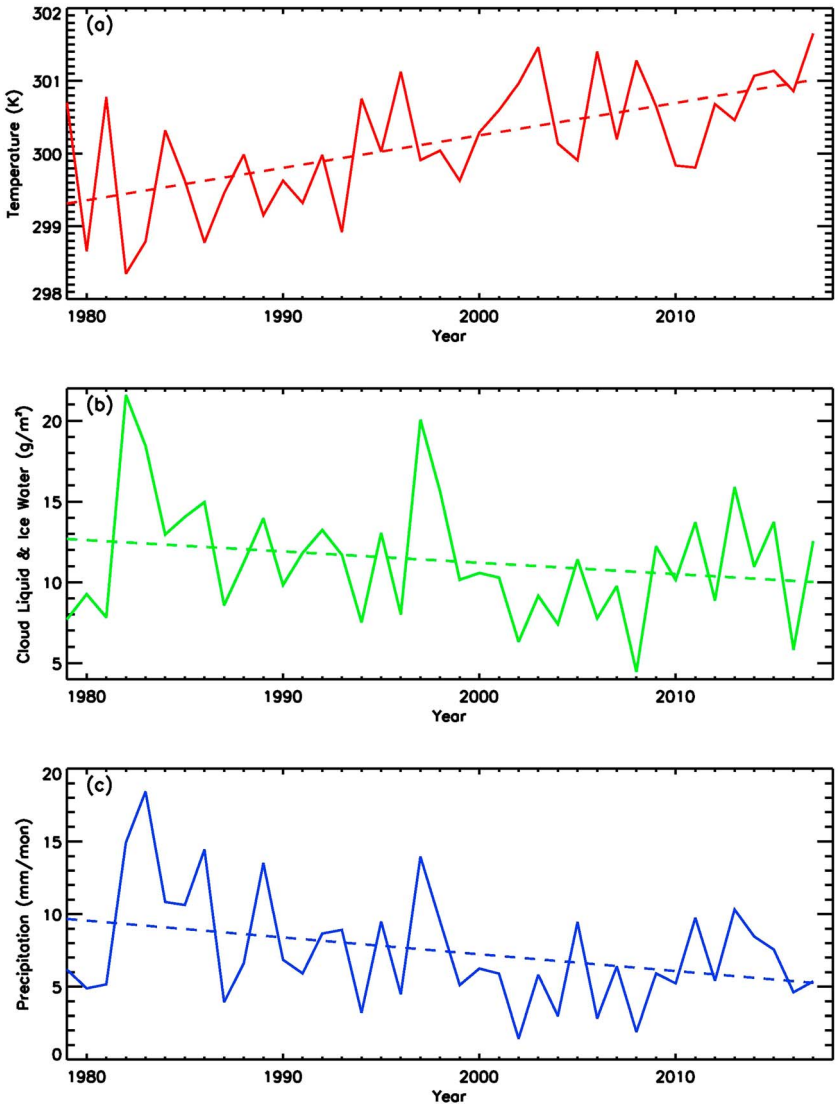

Figure 1. (a) ECMWF-Interim surface temperature averaged in California over the summer season (red solid line) and linear trend (red dashed line). Units are K. (b) ECMWF-Interim cloud liquid and ice path averaged in California over the summer season (green solid line) and linear trend (green dashed line). Units are g/m^2. (c) GPCP precipitation averaged in California over the summer season (blue solid line) and linear trend (blue dashed line). Units are mm/month.

CO_2 in different areas. Here we will utilize satellite CO_2 products to investigate the impact of wildfires on atmospheric CO_2 in California.

2. Data

Surface temperature, surface pressure, cloud liquid and ice water contents, precipitation, zonal wind, meridional wind, and vertical wind are used to explore the meteorological conditions for the October 2017 California wildfires. Monthly mean surface temperature data, surface pressure data, surface zonal wind data, and surface meridional wind data from European Weather Centre (ECMWF) Interim (Dee et al., 2011) are utilized in this paper. Spatial resolutions of the ECMWF-Interim surface temperature data, surface pressure data, and surface wind data are 0.75° × 0.75° (latitude × longitude). It covers from January 1979 to present. Data can be downloaded at https://apps.ecmwf.int/datasets/data/interim-full-daily/levtype=sfc/ website. Monthly mean precipitation data from Global Precipitation Climatology Project (GPCP; Adler et al., 2012; Adler et al., 2018) are used to explore the variability of precipitation. Spatial resolutions of the GPCP version 2.3 precipitation data are 2.5° × 2.5° (latitude × longitude). It

Table 1
Trends of ECMWF-Interim Surface Temperature (T), ECMWF-Interim Cloud Liquid and Ice Contents (W), and GPCP Precipitation (P) Averaged in California Over the Summer Season (JJAS). Correlation Coefficients and Significance Levels Between Different Variables (Detrended ECMWF-Interim Surface Temperature, Detrended ECMWF-Interim Cloud Liquid and Ice Contents, and Detrended GPCP Precipitation)

Variables	Trend	Correlation coefficient (Significance level)
ECMWF T	0.045 ± 0.017 K/year	
ECMWF W	−0.07 ± 0.09 g/m^2/year	
GPCP P	−0.12 ± 0.09 mm/year	
ECMWF T and ECMWF W		−0.52 (0.1%)
ECMWF T and GPCP P		−0.52 (0.1%)
ECMWF W and GPCP P		0.89 (0.1%)

Note. ECMWF = European Centre for Medium range Weather Forecasts; GPCP = Global Precipitation Climatology Project.

covers from January 1979 to present. Data can be downloaded at https://www.esrl.noaa.gov/psd/data/gridded/data.gpcp website. Cloud liquid and ice water contents from ECMWF-Interim (Delanoe et al., 2011) are also used in this paper to explore cloud variability. Monthly mean 500-hPa vertical velocity data from ECMWF-Interim (Dee et al., 2011) are used to explore the vertical transport. The spatial resolutions for ECMWF-Interim cloud water contents and vertical velocity are 0.75° × 0.75° (latitude × longitude). Data are available from January 1979 to present.

Monthly mean CO_2 data from Orbiting Carbon Observatory 2 (OCO-2) are used to explore the impact of wildfires on atmospheric CO_2. The OCO-2 satellite was launched in September 2014 (Crisp et al., 2017; Eldering et al., 2017). Two CO_2 absorption bands at 1.61 and 2.06 μm were used to estimate the column CO_2 dry-air mole fraction, X_{CO2}, using physical retrieval methods described in O'Dell et al. (2012) and Connor et al. (2008). The difference between OCO-2 X_{CO2} retrievals with the Total Carbon Column Observing Network measurements is less than 0.5 ppm with a standard deviation of 1.5 ppm (Wunch et al., 2017). The spatial resolutions of the OCO-2 CO_2 data are 1.29 km × 2.25 km. OCO-2 X_{CO2} retrievals can be downloaded at https://oco.jpl.nasa.gov/science/OCO2DataCenter/ website. We have regridded OCO-2 X_{CO2} data to 2° × 2° (latitude × longitude).

Moderate Resolution Imaging Spectrometer (MODIS) Climate Modeling Grid Burned Area products (Giglio et al., 2018) are used in this paper to explore burned areas in October 2017. MODIS burned areas are created using an updated burned area mapping algorithm from Giglio et al. (2016). The spatial resolutions of MODIS Climate Modeling Grid Burned Area product are 0.25° × 0.25° (latitude × longitude). Monthly mean MODIS burned area data are available from November 2000 to present. MODIS burned area data can be downloaded at ftp://fuoco.geog.umd.edu/MCD64CMQ/C6/ website.

3. Results

As a characteristic of the typical Mediterranean climate, there is usually more precipitation in the winter season and less precipitation in the summer season in California. In 2017, there was more precipitation in January to April, which triggered a massive growth of weeds/vegetation. These weeds/vegetation were dried out later on and became fuels for the wildfires in October 2017. There is a severe drought in June to September of 2017, which help produce favorable conditions for the wildfire in October 2017. To better explore possible reasons and favorable conditions for the California wildfire in October 2017, we examine the long-term trends of surface temperature, cloud liquid and ice water contents, and precipitation during the summer season (June–September) from 1979 to 2017. The whole summer season, which is just before the October 2017 wildfires, is chosen because we want to study the cumulative effect of the whole season on the formation of the October 2017 wildfires. The averaged ECMWF-Interim surface temperature (red line) in California in the summer season (June–September) is calculated in Figure 1a. The linear trend of the mean surface temperature is estimated by a multiple regression method (Bevington & Robinson, 2003; Li et al., 2011) and shown as red dashed line in Figure 1a. The linear trend of ECMWF-Interim surface temperature in California is about 0.043 ± 0.015 K/year. Over the past 39 years, the surface temperature of California has increased as a total of ~1.7 K in response to increasing greenhouse gases. The uncertainty of the trend is estimated by the standard deviation and degrees of freedom of the data (Bevington & Robinson, 2003; Box et al., 2005; Li et al., 2011). Details for the trend are summarized in Table 1.

During the summer, an increase in surface temperature coupled with changes in cloud water contents and precipitation lead to more severe droughts. To better understand the problem, we investigate ECMWF-Interim cloud liquid and ice water contents in California in the summer season (June–September, JJAS) from 1979 to 2017 (Figure 1b). Cloud water path including both liquid and ice water contents represent the total abundance of water in clouds per unit area. The cloud water path in California exhibits a weak linear trend of −0.07 ± 0.09 g/m^2/year in the past 39 years. Such a negative trends may explain less rain and

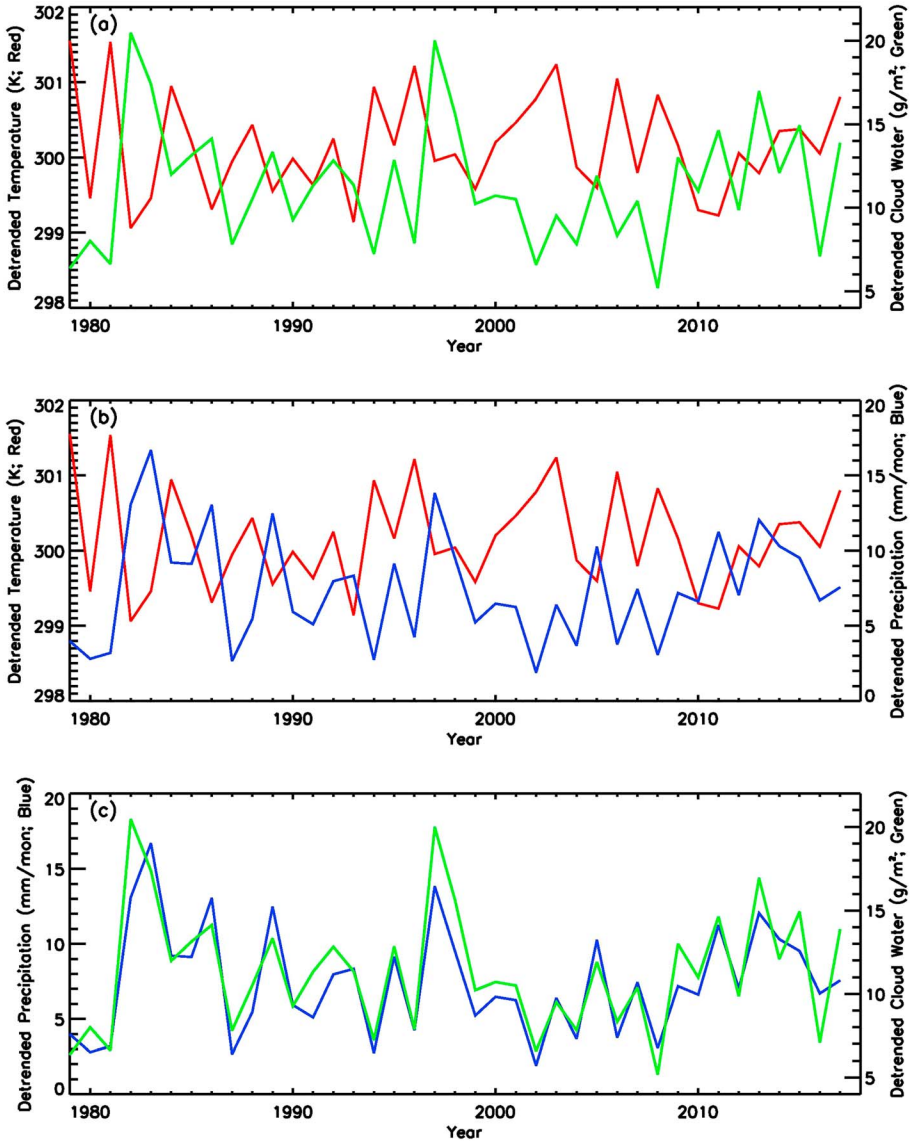

Figure 2. (a) Time series of detrended ECMWF-Interim summer surface temperature in California (red solid line) and detrended ECMWF-Interim summer cloud liquid and ice contents in California (green solid line). (b) Time series of detrended ECMWF-Interim summer surface temperature in California (red solid line) and detrended GPCP summer precipitation in California (blue solid line). (c) Time series of detrended GPCP summer precipitation in California (blue solid line) and detrended ECMWF-Interim summer cloud liquid and ice contents in California (green solid line).

therefore more droughts in recent years in California. To characterize the correlation between liquid/ice water contents and precipitation in California, we also explore the variation of precipitation in California in the summer season (JJAS) in California from 1979 to present, which is based on the datasets of GPCP version 2.3 precipitation. As shown in Figure 1c, the linear trend of GPCP summer precipitation in California is -0.12 ± 0.09 mm/year, which suggests that there is less rain in California in recent years.

To better explore the relationships among surface temperature, cloud water content, and precipitation, we compare the detrended time series of these variables in Figure 2. Linear trends have been removed from the raw data. Then the mean value for the raw data is added back to the detrended time series, so it is easier to compare with Figure 1. Time series of detrended surface temperature, detrended cloud water content, and detrended precipitation in summer season (JJAS) are shown in Figure 2. There is a negative correlation between detrended ECMWF-Interim summer surface temperature and detrended ECMWF-Interim summer cloud liquid and ice contents as shown in Figure 2a. The correlation coefficient between detrended ECMWF-

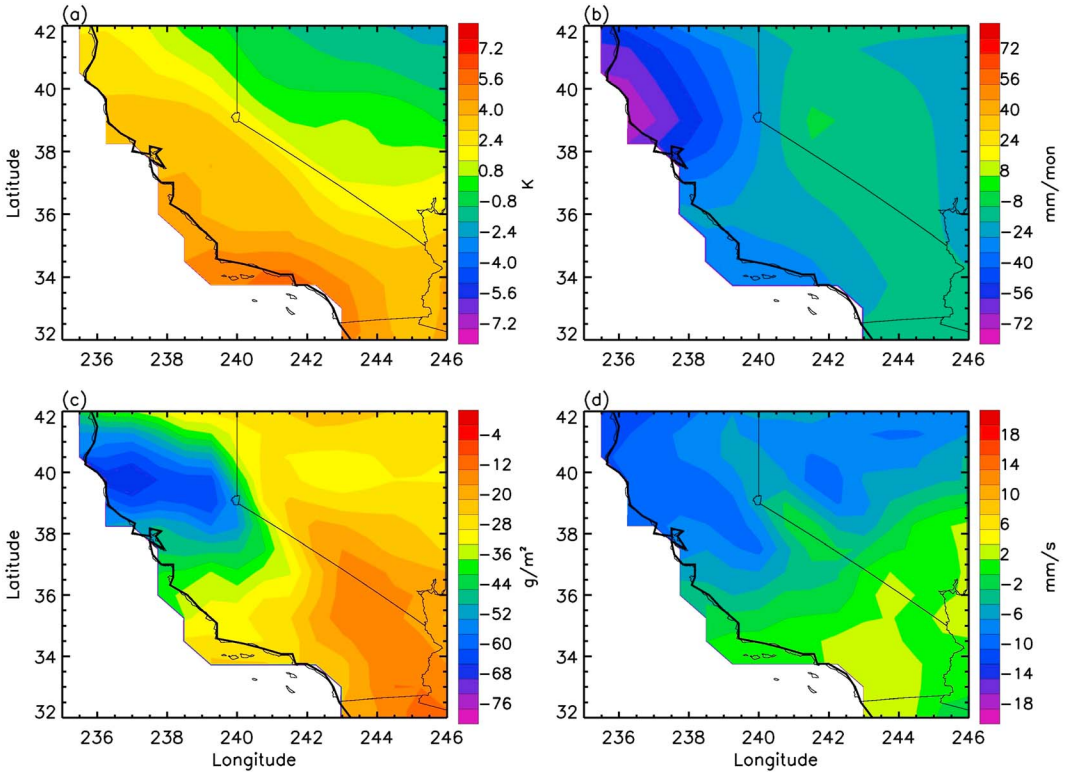

Figure 3. (a) ECMWF-Interim surface temperature anomaly in October 2017. Units are K. (b) GPCP precipitation anomaly in October 2017. Units are mm/month. (c) ECMWF-Interim cloud ice and liquid water anomaly in October 2017. Units are g/m^2. (d) ECMWF-Interim 500-hPa vertical velocity anomaly in October 2017. Units are mm/s.

Interim summer surface temperature and detrended ECMWF-Interim summer cloud water contents is −0.52 with a significance level of 0.1%. The significance level of the correlation coefficient is estimated using a Monte Carlo method (Jiang et al., 2004; Press et al., 1992). Time series of detrended ECMWF-Interim summer surface temperature and detrended GPCP summer precipitation are shown in Figure 2b. The correlation coefficient between detrended summer surface temperature and detrended summer precipitation is −0.52 (0.1%). The negative correlations between temperature, cloud water content, and precipitation are consistent with dry-get-dryer mechanism from the thermodynamical perspective. There is a positive correlation coefficient of 0.89 (0.1%) between detrended summer precipitation and detrended summer cloud water contents in California, suggesting that precipitation is closely related to the cloud liquid and ice water contents.

Since natural variability, such as El Niño and Pacific Decadal Oscillation (PDO), can influence precipitation as suggested by previous studies (e.g., Ashok et al., 2007; Gu & Adler, 2012; Marvel & Bonfils, 2013; Smith et al., 2006; Trammell et al., 2016), we also explore possible relationships among summer precipitation in California, El Niño, and PDO. Southern Oscillation Index (SOI) and PDO indices are used to represent the strengths of El Niño and PDO. Results between summer precipitation and SOI are shown in Figure S1 in the supporting information. As shown in Fig. S1a, summer precipitation has a negative trend of −0.12 ± 0.09 mm/year and SOI has a weak positive trend of 0.015 ± 0.034/year. Detrended summer precipitation and detrended SOI are shown in Fig. S1b. The correlation coefficient of detrended summer precipitation and detrended summer SOI is −0.04 (58.9%), which suggests that there is no clear relationship between summer precipitation and SOI. This might be explained by the fact that the summer season is the dry season for California and low precipitation can be influenced by different factors, such as cloud, surface temperature, and circulation. We also explore for a possible relationship between summer precipitation and PDO index, and do not notice any significant correlation between summer precipitation and PDO index.

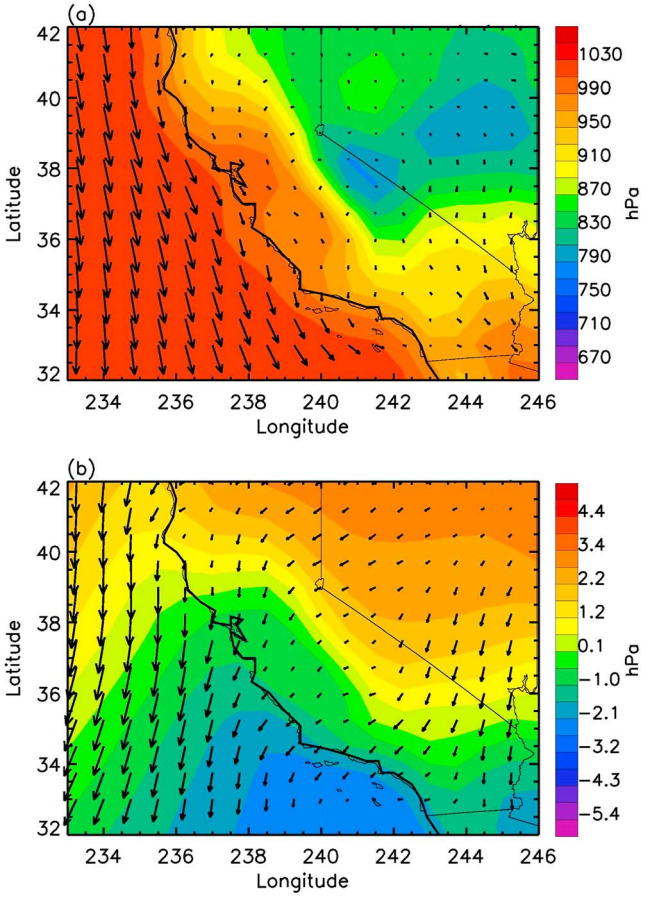

Figure 4. (a) ECMWF-Interim surface pressure and surface winds in October 2017. (b) ECMWF-Interim surface pressure anomalies and surface wind anomalies in October 2017. Units for surface pressure are hPa. For visualization, the longest (u, v) vector's length is 1.0 in each panel.

We investigate the spatial patterns of ECMWF-Interim surface temperature anomaly, GPCP precipitation anomaly, ECMWF-Interim cloud water content anomaly, and ECMWF-Interim 500-hPa vertical velocity anomaly at California in October 2017. Climatological values averaged from January 1979 to October 2017 have been removed from these variables. As shown in Figure 3a, there are positive temperature anomalies in California in October 2017, which agree with our previous finding about the increasing decadal trend of surface temperature in California. Meanwhile, there are negative precipitation anomalies in California in Octber 2017 (Figure 3b), especially in northern California. The negative precipitation anomalies are further related to the negative anomalies of cloud liquid and ice water path in California (Figure 3c). Convection and the related vertical motion also play important roles in the formation of precipitation. Hence, we also investigate the ECMWF-Interim 500-hPa vertical velocity, which is an index for the large-scale ascending/descending motion in the atmosphere and tightly related to precipitation (Kao et al., 2018). The reanalysis data shows that there are negative vertical velocity anomalies in California, suggesting strong sinking air in California in October 2017. The strong sinking air enhances the atmospheric stability and does not favor the formation of precipitation, leading to less precipitation in California in October 2017.

Since Pacific high pressure and horizontal winds can influence the weather in California, we explore the spatial distributions of surface pressure and surface winds in California in Figure 4. Monthly mean surface pressure and surface winds are shown in Figure 4a. The high pressure at Pacific Ocean tends to move moist air away from California. In the meanwhile, the Santa Ana winds tend to blow dry inland air to California. Both the high pressure and Santa Ana winds contribute to the drought in California in October 2017. Surface pressure anomalies and surface wind anomalies are shown in Figure 4b. There are positive pressure anomalies over the northern part and negative pressure anomalies over the southern part, which steepen the pressure gradient force and induces stronger northerly and northeast winds. As shown in Figure 4b, there are anomalies in the northerly winds near the California coast, which blocks the moist air away from California. There are also strong northerly winds and northeast winds over the land, which bring dry air from inland to California and contribute to the drought in this region. There are about 15 destructive fire events in October 2017 with the burnt area exceeding 1,000 acres. Four fire events are among the twenty most destructive wildfires in California's history. These four fire events are Tubbs fire (Napa and Sonoma County), Nuns fire (Sonoma County), Atlas (Napa and Solano County), and Redwood Valley Complex (Mendocino County), which occurred in the northern California. As shown in Figure 4, there are anomalous northerly winds and northeast winds over northern California, which bring dry air from inland to these areas. There are also strong wild fires occurring in southern California, such as Canyon 2 fire (Orange County), Buffalo fire (San Diego County), and Wildomar fire (Riverside County). There are anomalous northerly winds in Southern California, which bring dry air to Southern California. The analyses of time series and spatial patterns both suggest that the positive surface temperature, negative precipitation, negative cloud water contents, enhanced sinking air, Pacific high pressure, and enhanced Santa Ana winds contribute to drought conditions in California, which further induces the October 2017 wildfires in California.

In addition to exploring the favorable conditions for the October 2017 wildfires in California, we also assess the impact of wildfires on atmospheric CO_2. It is well known that wildfires release CO_2 into the atmosphere through the combustion processes of organic matter. The newly retrieved global CO_2 data sets from the satellite OCO-2 (Crisp et al., 2017) provide us a great opportunity to examine the increase in the atmospheric CO_2 from one of the largest wildfires in California's history.

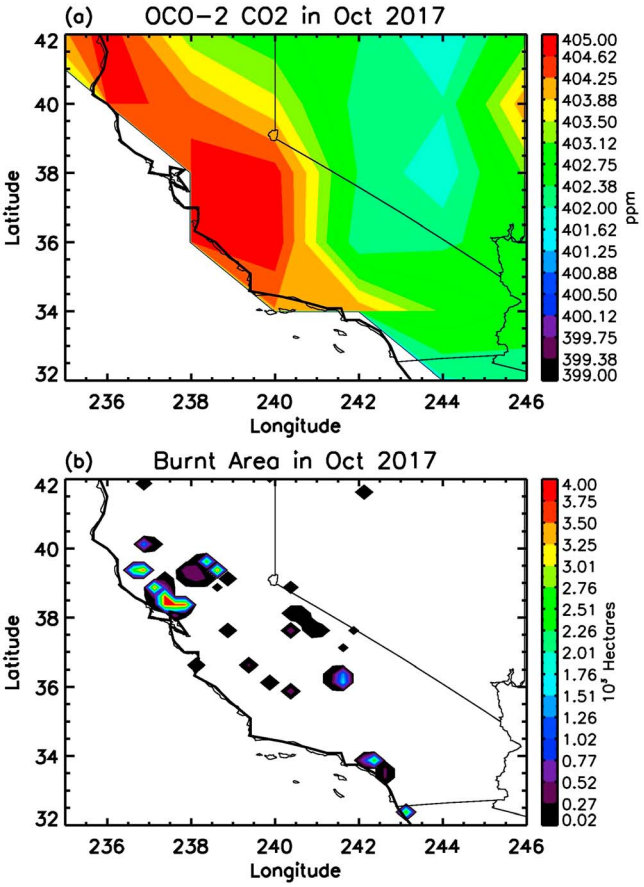

Figure 5. (a) OCO-2 CO_2 in October 2017. Units are ppm. (b) MODIS burned area in October 2017. Units are 10^3 hectares.

Monthly mean OCO-2 column CO_2 data in October 2017 is shown in Figure 5a, which shows that more than 2-ppm CO_2 is released to the atmosphere in California during the October 2017 wildfires compared with surrounding states (e.g., Nevada). MODIS burned areas in October 2017 are shown in Figure 5b. The major fire events in October 2017 can be identified in Figure 5b. The CO_2 increase due to the largest wildfires is comparable to the magnitude of the long-term CO_2 trend (~2 ppm/year) induced by human activities. Such a significant CO_2 source needs to be considered in the current studies of environment and model simulation. Previous study (Saha et al., 2017) also found that the fire can increase albedo and latent heat, which leads to less convective precipitation. As suggested in Saha et al. (2017), the brightening after fire as a result of drier soils and losing senescent vegetation is responsible for rainfall suppression. It will further lead to more severe droughts and wildfires in California in the future, which will release more CO_2 to the atmosphere.

4. Conclusion

The October 2017 California wildfires were one of the largest wildfires in the state's history. The averaged surface temperature in the summer season (JJAS) in California has increased by 1.7 K during the past 39 years (1979–2017) as suggested by the ECMWF-Interim Reanalysis data. Meanwhile, both summer precipitation and summer cloud liquid and ice water contents decrease with time in California. The decreasing precipitation contributes to more severe droughts in the region and further favors the wildfires in California.

Our investigation of the anomalies of surface temperature, surface pressure, precipitation, cloud water contents, surface horizontal winds, and 500-hPa vertical velocity in October 2017 suggests significant correlations and possible causality among high temperature, surface pressure, low precipitation, low cloud water contents, enhanced surface Santa Ana winds, and enhanced sinking air in California. All of these factors contribute to more severe droughts, which can contribute to stronger and more devastating wildfires.

We also quantify the release of CO_2 from the largest wildfires in California's history for the first time. As suggested by the OCO-2 satellite CO_2 data, there is ~2 ppm more CO_2 released to the atmosphere by the October 2017 wildfires. Considering that CO_2 released from wildfires may keep increasing, we have to carry out more stringent control policy and curb more emissions of CO_2 from other anthropogenic sources (e.g., industrial and automobile; Newman et al., 2016) to mitigate global warming. As a positive feedback, effective control of anthropogenic CO_2 can help us prevent future wildfires in California and other areas.

Acknowledgments
We thank two anonymous referees and editor for their time and constructive suggestions. We thank helpful comments from Sally Newman and William Chan. Y. Y. is supported by the NASA OCO-2 project. Y. W. acknowledges the support from AQ-SRTD at Jet Propulsion Laboratory and Multi-Angle Imager for Aerosols project. ECMWF-Interim data can be downloaded at https://apps.ecmwf.int/datasets/data/interim-full-daily/levtype=sfc/ website. GPCP precipitation data can be downloaded at https://www.esrl.noaa.gov/psd/data/gridded/data.gpcp website. OCO-2 X_{CO2} retrievals can be downloaded at https://oco.jpl.nasa.gov/science/OCO2DataCenter/ website. MODIS burned area data can be downloaded at ftp://fuoco.geog.umd.edu/MCD64CMQ/C6/ website.

References

Adler, R. F., Gu, G. J., & Huffman, G. J. (2012). Estimating climatological bias errors for the Global Precipitation Climatology Project (GPCP). *Journal of Applied Meteorology and Climatology*, *51*(1), 84–99. https://doi.org/10.1175/JAMC-D-11-052.1

Adler, R. F., Sapiano, M., Huffman, G., Wang, J.-J., Gu, G., Bolvin, D., et al. (2018). The Global Precipitation Climatology Project (GPCP) monthly analysis (New Version 2.3) and a review of 2017 global precipitation. *Atmosphere*, *9*(4). https://doi.org/10.3390/atmos9040138

Allan, R. P., & Soden, B. J. (2007). Large discrepancy between observed and simulated precipitation trends in the ascending and descending branches of the tropical circulation. *Geophysical Research Letters*, *34*, L18705. https://doi.org/10.1029/2007GL031460

Ashok, K., Behera, S. K., Rao, S. A., Weng, H., & Yamagata, T. (2007). El Niño Modoki and its possible teleconnection. *Journal of Geophysical Research*, *112*. https://doi.org/10.1029/2006JC003798

Balling, R. C., Meyer, G. A., & Wells, S. G. (1992). Climate Change in Yellowstone National Park: Is the drought-related risk of wildfires increasing. *Climate Change*, *22*(1), 35–45. https://doi.org/10.1007/BF00143342

Bevington, P. R., & Robinson, D. K. (2003). *Data reduction and error analysis for the physical sciences* (3rd ed., p. 320). New York: McGraw_Hill.

Box, G. E. P., Hunter, J. S., & Hunter, W. G. (2005). *Statistics for experiments: Design, innovation, and discovery* (2nd ed., p. 664). New York: John Wiley & Sons.

Cai, C., Kulkarni, S., Zhao, Z., Kaduwela, A. P., Avise, J. C., DaMassa, J. A., et al. (2016). Simulating reactive nitrogen, carbon monoxide, and ozone in California during ARCTAS-CARB 2018 with high wildfire activity. *Atmospheric Environment*, *128*, 28–44. https://doi.org/10.1016/j.atmosenv.2015.12.031

Chou, C., & Neelin, J. D. (2004). Mechanisms of global warming impacts on regional tropical precipitation. *Journal of Climate*, *17*(13), 2688–2701. https://doi.org/10.1175/1520-0442(2004)017<2688:MOGWIO>2.0.CO;2

Connor, B. J., Boesch, H., Toon, G., Sen, B., Miller, C., & Crisp, D. (2008). Orbiting Carbon Observatory: Inverse method and prospective error analysis. *Journal of Geophysical Research*, *113*, D05305. https://doi.org/10.1029/2006JD008336

Crisp, D., Pollock, H. R., Rosenberg, R., Chapsky, L., Lee, R. A. M., Oyafuso, F. A., et al. (2017). The on-orbit performance of the Orbiting Carbon Observatory-2 (OCO-2) instrument and its radiometrically calibrated products. *Atmospheric Measurement Techniques*, *10*(1), 59–81. https://doi.org/10.5194/amt-10-59-2017

Crockett, J. L., & Westerling, A. L. (2018). Greater temperature and precipitation extremes intensify western U.S. droughts, wildfire severity, and Sierra Nevada tree mortality. *Journal of Climate*, *31*(1), 341–354. https://doi.org/10.1175/JCLI-D-17-0254.1

Dee, D. P., Uppala, S. M., Simmons, A. J., Berrisford, P., Poli, P., Kobayashi, S., et al. (2011). The ERA-Interim reanalysis: Configuration and performance of the data assimilation system. *Quarterly Journal of the Royal Meteorological Society*, *137*(656), 553–597. https://doi.org/10.1002/qj.828

Delanoe, J., Hogan, R. J., Forbes, R. M., Bodas-Salcedo, A., & Stein, T. H. M. (2011). Evaluation of ice cloud representation in the ECMWF and UK Met Office models using CloudSat and CALLPSO data. *Quarterly Journal of the Royal Meteorological Society*, *137*(661), 2064–2078. https://doi.org/10.1002/qj.882

Eldering, A., O'Dell, C. W., Wennberg, P. O., Crisp, D., Gunson, M. R., Viatte, C., et al. (2017). The Orbiting Carbon Observatory-2: First 18 months of science data products. *Atmospheric Measurement Techniques*, *10*(2), 549–563. https://doi.org/10.5194/amt-10-549-2017

Giglio, L., Boschetti, L., Roy, D., Hoffmann, A. A., Humber, M., & Hall, J. V. (2018). Collection 6 MODIS burned area product user's guide version 1.2.

Giglio, L., Schroeder, W., & Justice, C. O. (2016). The collection 6 MODIS active fire detection algorithm and fire products. *Remote Sensing of Environment*, *178*, 31–41. https://doi.org/10.1016/j.rse.2016.02.054

Griffin, D., & Anchukaitis, K. J. (2014). How unusual is the 2012–2014 California drought. *Geophysical Research Letters*, *41*, 9017–9023. https://doi.org/10.1002/2014GL062433

Gu, G. J., & Adler, R. F. (2012). Interdecadal variability/long term changes in global precipitation patterns during the past three decades: Global warming and/or Pacific decadal variability. *Climate Dynamics*, *40*(11-12), 3009–3022. https://doi.org/10.1007/s00382-012-1443-8

Guyon, P., Frank, G. P., Welling, M., Chand, D., Artaxo, P., Rizzo, L., et al. (2005). Airborne measurements of trace gas and aerosol particle emissions from biomass burning in Amazonia. *Atmospheric Chemistry and Physics*, *5*(11), 2989–3002. https://doi.org/10.5194/acp-5-2989-2005

Heymann, J., Reuter, M., Buchwitz, M., Schneising, O., Bovensmann, H., Burrows, J. P., et al. (2017). CO_2 emission of Indonesian fires in 2015 estimated from satellite-derived atmospheric CO_2 concentrations. *Geophysical Research Letters*, *44*, 1537–1544. https://doi.org/10.1002/2016GL072042

Intergovernment Panel on Climate Change (2013). *Climate Change 2013: The Physical Science Basis*. Geneva, Switzerland: IPCC Secretariat, World Meteorological Organization.

Jiang, X., Camp, C. D., Shia, R., Noone, D., Walker, C., & Yung, Y. L. (2004). Quasi-biennial oscillation and quasi-biennial oscillation-annual beat in the tropical total column ozone: A two-dimensional model simulation. *Journal of Geophysical Research*, *109*, D16305. https://doi.org/10.1029/2003JD004377

Kao, A., Jiang, X., Li, L., Su, H., & Yung, Y. L. (2017). Precipitation, circulation, and cloud variability over the past two decades. *Earth and Space Science*, *4*, 597–606. https://doi.org/10.1002/2017EA000319

Kao, A., Jiang, X., Li, L., Trammell, J. H., Zhang, G. J., Su, H., et al. (2018). A comparative study of atmospheric moisture recycling rate between observations and models. *Journal of Climate*, *31*(6), 2389–2398. https://doi.org/10.1175/JCLI-D-17-0421.1

Li, L., Jiang, X., Chahine, M. T., Olsen, E. T., Fetzer, E. J., Chen, L., & Yung, Y. L. (2011). The recycling rate of atmospheric moisture over the past two decades (1988-2009). *Environmental Research Letters*, *6*(3). https://doi.org/10.1088/1748-9326/6/3/034017.

Marvel, K., & Bonfils, C. (2013). Identifying external influences on global precipitation. *Proceedings of the National Academy of Sciences of the United States of America*, *110*(48), 19301–19306. https://doi.org/10.1073/pnas.1314382110

Newman, S., Xu, X., Gurney, K. R., Hsu, Y. K., Li, K. F., Jiang, X., et al. (2016). Toward consistency between trends in bottom-up CO_2 emissions and top-down atmospheric measurements in the Los Angeles megacity. *Atmospheric Chemistry and Physics*, *16*(6), 3843–3863. https://doi.org/10.5194/acp-16-3843-2016

O'Shea, S., Allen, G., Gallagher, M. W., Bauguitte, S. J.-B., Illingworth, S. M., Le Breton, M., et al. (2013). Airborne observations of trace gases over boreal Canada during BORTAS: Campaign climatology, air mass analysis and enhancement ratios. *Atmospheric Chemistry and Physics*, *13*, 12451–12467.

O'Dell, C., Connor, B., Bösch, H., O'Brien, D., Frankenberg, C., Castano, R., et al. (2012). The ACOS CO_2 retrieval algorithm-Part I: Description and validation against synthetic observations. *Atmospheric Measurement Techniques*, *5*, 99–121.

Pausas, J. G., & Fernandez-Munoz, S. (2012). Fire regime changes in the Western Mediterranean Basin: From fuel-limited to drought driven fire regime. *Climate Change*, *110*(1-2), 215–226. https://doi.org/10.1007/s10584-011-0060-6

Polson, D., Hegerl, G. C., Allan, R. P., & Balan Sarojini, B. (2013). Have greenhouse gases intensified the contrast between wet and dry regions. *Geophysical Research Letters*, *40*, 4783–4787. https://doi.org/10.1002/grl.50923

Press, W., Teukolsky, S., Vetterling, W., & Flannery, B. (1992). *Numerical recipes in Fortran 77: The art of scientific computing* (2nd ed., p. 933). New York: Cambridge University Press.

Saha, M. V., D'Odorico, P., & Scanlon, T. M. (2017). Albedo Changes after fire as an explanation of fire-induced rainfall suppression. *Geophysical Research Letters*, *44*, 3916–3923. https://doi.org/10.1002/2017GL073623

Santer, B. D., Mears, C., Wentz, F. J., Taylor, K. E., Gleckler, P. J., Wigley, T. M. L., et al. (2007). Identification of human-induced changes in atmospheric moisture content. *Proceedings of the National Academy of Sciences of the United States of America*, *104*(39), 15248–15253. https://doi.org/10.1073/pnas.0702872104

Smith, T., Yin, X., & Gruber, A. (2006). Variations in annual global precipitation (1979–2004), based on the Global Precipitation Climatology Project 2.5 analysis. *Geophysical Research Letters*, *33*, L06705. https://doi.org/10.1029/2005GL025393

Su, H., Jiang, J. H., Neelin, J. D., Shen, T. J., Zhai, C., Yue, Q., et al. (2017). Tightening of tropical ascent and high clouds key to precipitation change in a warmer climate. *Nature Communications*, *8*(1), 15771. https://doi.org/10.1038/ncomms15771

Trammell, J. H., Jiang, X., Li, L., Kao, A., Zhang, G. J., Chang, E. K. M., & Yung, Y. (2016). Temporal and spatial variability of precipitation from observations and models. *Journal of Climate*, *29*(7), 2543–2555. https://doi.org/10.1175/JCLI-D-15-0325.1

Trammell, J. H., Jiang, X., Li, L., Liang, M., Li, M., Zhou, J., et al. (2015). Investigation of precipitation variations over wet and dry areas from observation and model. *Advances in Meteorology*, 981092.

Trenberth, K. E., Fasullo, J., & Smith, L. (2005). Trends and variability in column-integrated atmospheric water vapor. *Climate Dynamics*, *24*, 741–758.

Wang, Y., Ma, P. L., Jiang, J., Su, H., & Rasch, P. (2016). Towards reconciling the influence of atmospheric aerosols and greenhouse gases on light precipitation changes in Eastern China. *Journal of Geophysical Research: Atmospheres*, *121*, 5878–5887. https://doi.org/10.1002/2016JD024845

Wunch, D., Wennberg, P. O., Osterman, G., Fisher, B., Naylor, B., Roehl, C. M., et al. (2017). Comparisons of the Orbiting Carbon Observatory-2 (OCO-2) XCO_2 measurements with TCCON. *Atmospheric Measurement Techniques*, *10*(6), 2209–2238. https://doi.org/10.5194/amt-10-2209-2017